Indian Journal of Pure & Applied Physics
Vol. 60, January 2022, pp. 78-89

# Nanofluid Bioconvection in Porous Enclosure with Viscous Dissipation

Ramesh Alluguvelli[a*], Chandra Shekar Balla[b], Kishan Naikoti[c] & Oluwole Daniel Makinde[d]

[a]Department of Mathematics, Geethanjali College of Engineering and Technology, Affiliated to JNTUH, Hyderabad 501 301, India

[b]Department of Mathematics, Chaitanya Bharathi Institute of Technology, Affiliated to Osmania University, Hyderabad 500 075, India

[c]Department of Mathematics, Osmania University 500 007, Hyderabad, India

[d]Faculty of Military Science, Stellenbosch University, Private Bag X1 MATIELAND 7602 South Africa

*Received 7 March 2020; accepted 16 November 2021*

In this paper, the bioconvective nanofluid flow in porous square enclosure containing oxytactic microorganism associated with viscous dissipation, is discussed. The bioconvection flow in porous medium is framed by Darcy-Boussinesq approximation. Galerkin finite elements method is employed to solve the governed equations. The computational numerical results are exhibited by the surface plots of stream function, temperature, concentration of oxygen and microorganisms, average Nusselt number, average Sherwood numbers of oxygen and microorganism concentrations. The effects of key parameters such as Peclet number (Pe), Rayleigh number of bioconvection (Rb), viscous dissipation (Ec), thermophoretic parameter (Nt), parameter of Brownian movement (Nb), Lewis number (Le) and Rayleigh number (Ra) are presented and analyzed.

**Keywords**: Thermo-bioconvection; Oxytactic microorganisms; Thermophoetic force; Square enclosure in porous medium; Viscous dissipation; Peclet number; Brownian motion

## 1 Introduction

Abundant investigations on convection and heat transfer through porous media are ascribed to the enormous of applications, such as utilization and storage of thermal/geothermal energy, reservoirs of petroleum, devices of catalytic convertors, dispersion of underground pollutants, underground feeder cables, technology of porous ceramic burners, food industry, tertiary recovery, chemical reactors, chemical separations, moisture migration in stored grain, thermal cooling of electronic equipment, heating of rooms, combustion. The basic nature and increased volume of research in concerned discipline are adequately archived by Nield and Bejan[1], Vafai[2], Pop and Ingham[3]. Natural convection in cavities of various geometries discovers a salient feature for the analysis of engineering. It has huge applications in solar energy, cooling system for buildings, electronics industry, etc. Many authors have examined the natural convection phenomenon in a porous square cavity [4–8].

A latest development for microfluidic devices is bioconvective heat transfer in porous media. It refers to a macroscopic convective movement of fluid induced by swimming of motile microorganisms. Different types of microorganisms showing various swimming behaviors, can be found. Microorganisms of negative geotaxis swim opposite to gravity[9]. The swimming trend of gyrotactic microorganisms depend on the balance of gravitational and viscous forces[10,11]. Generally, oxytactic microorganisms swim towards the upper surface since the upper surface of any layer is opened to the atmosphere wherever the oxygen density is abundant. Growth of microorganisms at the upper surface generates the inverting instability, which leads to the formation of bioconvection. Hillesdon *et al.*[12] and Hillesdon and Pedley[13] developed the theoretical model of bioconvection due to oxytactic micro-organisms. Many authors studied the onset thermobioconvection containing oxytactic microorganisms[14–17]. Kuznetsov[18] presented a continuum model for thermobioconvection of oxytactic micro-organisms in porous media and examined the mixed consequences of up swimming of bacteria and heat transfer below horizontal porous layer. Ahmed *et al.*[19] investigated thermo-bioconvection in a homogeneous and isotropic porous medium saturated square enclosure containing oxytactic microorganisms.

The emerging area of nanofluids has gained substantial attention by research community owing to its outstanding attribute of enhancing the thermal conductivity comparative to base fluids. This concept

*Corresponding author: (E-mail: alluramesh1@gmail.com)

was developed by Choi and Eastman[20]. Many researchers [21–25] contributed to nanofluid flow in various geometries of Brownian motion model and nanoparticle-volume fraction model as well. The applications of nanofluids with microorganisms can be found in micromixers, micro reactors, enzyme biosensors, construction of chip-size micro devices, heat sinks of micro heat cylinder and micro channel[26–31]. The medical and biotechnological applications which need comprehension of fluids containing nanofluid with micro-organisms in porous media include micropumps[32], transportation in microfluidics[33], microbial enhanced oil recovery, applied to improve the span of matured oil reservoirs[34–36]. Beg *et al.* [37] employed a mathematical model for nano-bioconvection past an impermeable vertical porous flat wall filled with oxytactic microorganisms. Balla *et al.*[38] examined the impact of bioconvection parameters in suspensions of oxytactic microorganisms present in porous medium.

Effect of viscous dissipation is producing local thermal energy through the mechanism of viscous stresses that affects convective flow and rate of heat transfer. kefene *et al.*[39] presented MHD variable viscosity mixed convection of nanofluid in a microchannel with permeable walls. Chaudhary *et al.*[40] studied the effects of viscous dissipation and radiation on unsteady incompressible fluid flow through a porous media with a magnetic field and heat generation/absorption. Several researchers[41–44] have focused their efforts on the influence of viscous dissipation in fluid-saturated porous medium, but very little attention is focused on evaluating this effect in nanofluids flowing past various surface geometries. Aziz *et al.*[45] and Sachin *et al.*[46] investigated nanofluid flow assisted by viscous dissipation effects past a porous plate containing gyrotactic micro-organisms. Gireesha *et al.*[47] studied the combined effects of viscous dissipative nanofluid flow of gyrotactic microorganisms over a stretching sheet. Hady *et al.*[48], Uddin *et al.*[49] and Khan *et al.*[50] analyzed the effects of Viscous dissipation on steady/unsteady thermo bioconvection containing gyrotactic microorganisms and nanoparticles.

A novel attempt is to combine the impacts of viscous dissipation and oxytactic microorganism in bioconvective nanofluid flow. To the best of authors' knowledge, the current work is not reported so far to the case of viscous dissipation of bioconvection due to motile oxytactic bacteria and nanoparticles in porous media. The combined effects of viscous dissipation and oxytactic microorganisms in square enclosure may serve as a considerable problem for future scope. The objective of current paper is to improve the work of Balla *et al.*[38] to the extent of oxytactic microorganisms and nanoparticles with the influence of viscous dissipation.

## 2 Mathematical Formulation

A bioconvective nanofluid flow in porous square enclosure filled by oxytactic microorganisms associated with viscous dissipation is considered. Assume that the right and left walls of the square enclosure whose length is $L$, are kept at temperatures $T_c$ and $T_H$ satisfying $T_H > T_c$ (see Fig. 1). The enclosure is assumed to have adiabatic bottom and top walls. The gravitational vector $g$ acts in negative direction to the y–axis. The equations of suspension containing oxytactic microorganisms rely on the mathematical formulation of Hillesdon and Pedley[13]. A dilute solution is presumed and terms of inertia are neglected owing to the extreme slow movement of bioconvection flow. In view of the Boussinesq approximation, governing equations are:

$$\frac{\partial u}{\partial x}+\frac{\partial v}{\partial y}=0 \qquad \ldots (1)$$

$$\frac{\mu}{K}u=-\frac{\partial p}{\partial x} \qquad \ldots (2)$$

$$\frac{\mu}{K}v=-\frac{\partial p}{\partial y}-\left[\gamma\Delta\rho n-\rho_f\ \beta(T-T_C)\right]g \qquad \ldots (3)$$

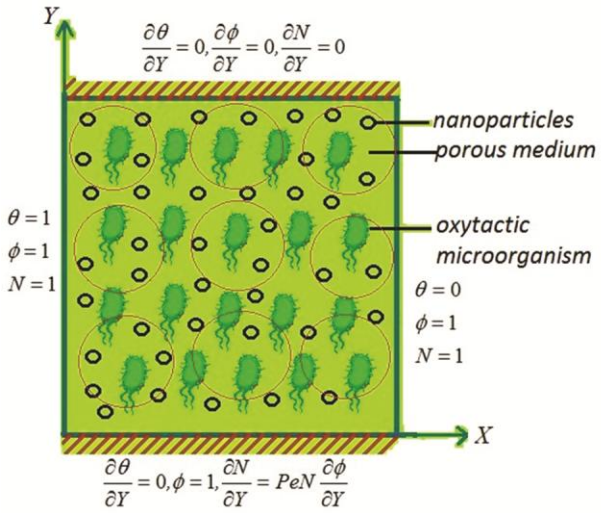


Fig. 1 — Geometry and physical configuration.

$$u\frac{\partial T}{\partial x}+v\frac{\partial T}{\partial y}=\alpha_m\left(\frac{\partial^2 T}{\partial x^2}+\frac{\partial^2 T}{\partial y^2}\right)+\frac{\mu}{K(\rho C_P)_f}\left(u^2+v^2\right)+\tau\left\{D_B\left(\frac{\partial C}{\partial x}\frac{\partial T}{\partial x}+\frac{\partial C}{\partial y}\frac{\partial T}{\partial y}\right)+\frac{D_T}{T_C}\left[\left(\frac{\partial T}{\partial x}\right)^2+\left(\frac{\partial T}{\partial y}\right)^2\right]\right\} \quad \text{... (4)}$$

$$u\frac{\partial C}{\partial x}+v\frac{\partial C}{\partial y}=D_B\left(\frac{\partial^2 C}{\partial x^2}+\frac{\partial^2 C}{\partial y^2}\right)-\delta n+\frac{D_T}{T_C}\left(\frac{\partial^2 T}{\partial x^2}+\frac{\partial^2 T}{\partial y^2}\right) \quad \text{... (5)}$$

$$\frac{\partial}{\partial x}\left[un+\tilde{u}n-D_n\frac{\partial n}{\partial x}\right]+\frac{\partial}{\partial y}\left[vn+\tilde{v}n-D_n\frac{\partial n}{\partial y}\right]=0 \quad \text{... (6)}$$

Here $\Delta C=C_0-C_{min}$. $D_n$ is the diffusivity of the microorganisms and $D_B$ is diffusivity of oxygen *n* is number density of motile microorganisms, $-\delta n$ accounts utilization of oxygen by the microorganism.

The terms $\tilde{u}$ , $\tilde{v}$ are as follow:

$$\tilde{u}=\left(\frac{bW_C}{\Delta C}\right)\frac{\partial C}{\partial x} \quad \text{... (7)}$$

and

$$\tilde{v}=\left(\frac{bW_C}{\Delta C}\right)\frac{\partial C}{\partial y} \quad \text{... (8)}$$

where *b* is constant of chemotaxis and *Wc* is maximum speed that cell swims.

Using following nondimensional variables

$$X=\frac{x}{L},Y=\frac{y}{L},\Psi=\frac{\psi}{\alpha_m},\theta=\frac{T-T_C}{\Delta T},\quad \phi=\frac{C-C_{min}}{\Delta C},N=\frac{n}{n_0} \quad \text{... (9)}$$

where $n_0$ represents averaged density of microorganism. Utilizing dimensional stream function $\Psi$, which is given by $u=\frac{\partial\psi}{\partial Y}$ and $v=-\frac{\partial\psi}{\partial x}$, the following non-dimensionalized equations are resulted.

$$\frac{\partial^2\Psi}{\partial X^2}+\frac{\partial^2\Psi}{\partial Y^2}=-Ra\left(\frac{\partial\theta}{\partial X}-Rb\frac{\partial N}{\partial X}\right) \quad \text{... (10)}$$

$$\frac{\partial\Psi}{\partial Y}\frac{\partial\theta}{\partial X}-\frac{\partial\Psi}{\partial X}\frac{\partial\theta}{\partial Y}=\frac{\partial^2\theta}{\partial X^2}+\frac{\partial^2\theta}{\partial Y^2}+Ec\left[\left(\frac{\partial\Psi}{\partial X}\right)^2+\left(\frac{\partial\Psi}{\partial Y}\right)^2\right]+Nb\left(\frac{\partial\phi}{\partial X}\frac{\partial\theta}{\partial X}+\frac{\partial\phi}{\partial Y}\frac{\partial\theta}{\partial Y}\right)+Nt\left[\left(\frac{\partial\theta}{\partial X}\right)^2+\left(\frac{\partial\theta}{\partial Y}\right)^2\right] \quad \text{... (11)}$$

$$\frac{\partial\Psi}{\partial Y}\frac{\partial\phi}{\partial X}-\frac{\partial\Psi}{\partial X}\frac{\partial\phi}{\partial Y}=\frac{1}{Le}\left(\frac{\partial^2\phi}{\partial X^2}+\frac{\partial^2\phi}{\partial Y^2}\right)-\frac{\sigma}{Le}N \quad \text{... (12)}$$

$$Le.\chi\left(\frac{\partial\Psi}{\partial Y}\frac{\partial N}{\partial X}-\frac{\partial\Psi}{\partial X}\frac{\partial N}{\partial Y}\right)+Pe\left[\frac{\partial}{\partial X}\left(N\frac{\partial\phi}{\partial X}\right)+\frac{\partial}{\partial Y}\left(N\frac{\partial\phi}{\partial Y}\right)\right]=\frac{\partial^2 N}{\partial X^2}+\frac{\partial^2 N}{\partial Y^2} \quad \text{... (13)}$$

where the parameters of Brownian motion (*Nb*), thermophoresis (*Nt*), bio convection Rayleigh number (*Rb*), Rayleigh number related to porous medium (*Ra*), Peclet number (*Pe*), Lewis number (*Le*), Eckert number (*Ec*) and parameter ($\sigma$) are given as

$$Ra=\frac{gK\beta\Delta TL}{\nu\alpha_m},Le=\frac{\alpha_m}{D_C},Rb=\frac{\gamma\Delta\rho n_0}{\rho_f\beta\Delta T},\chi=\frac{D_C}{D_n},\quad Pe=\frac{bW_C}{D_n},\sigma=\frac{\delta n_0 L^2}{D_C\Delta C},$$

$$Nb=\frac{\tau D_B\Delta C}{\alpha_m},Nt=\frac{\tau D_T(T_H-T_C)}{\alpha_m T_C},\quad Ec=\frac{\mu\alpha_m}{K\left(\rho C_P\right)_f\Delta T}$$

The dimensionless form of boundary conditions (10)-(13) are:

$$\Psi=0,\theta=1,\phi=1,N=1 \text{ at } X=0$$

$$\Psi=0,\theta=0,\phi=1,N=1 \text{ at } X=1$$

$$\Psi=0,\frac{\partial\theta}{\partial Y}=0,\phi=1,PeN\frac{\partial\phi}{\partial Y}=\frac{\partial N}{\partial Y} \text{ at } Y=0 \quad \text{... (14)}$$

$$\Psi=0,\frac{\partial\theta}{\partial Y}=0,\frac{\partial\phi}{\partial Y}=0,\frac{\partial N}{\partial Y}=0 \text{ at } Y=1$$

The local values of Nusselt number $Nu_Y$, Sherwood number of oxygen concentration $Sh_Y$, Sherwood number of microorganisms concentration $Nn_Y$ and their average values are defined by

$$Nu_Y=-\left(\frac{\partial\theta}{\partial X}\right)_{X=0,1},\ Sh_Y=-\left(\frac{\partial\phi}{\partial X}\right)_{X=0,1},\ Nn_Y=-\left(\frac{\partial N}{\partial X}\right)_{X=0,1}$$

and

$$Nu_{avg}=\int_0^1 Nu_Y dY\ ,\ Sh_{avg}=\int_0^1 Sh_Y dY,\ Nn_{avg}=\int_0^1 Nn_Y dY$$

## 3 Method of solution

Finite elements method of Galerkin's weighted residues procedure is employed to find solution of non-dimensionalised governing equations (10)-(13) with associated boundary conditions (14). In this scheme suitable trial solutions are deputed and residuals are collected. The product of residuals and weight functions is integrated over each element and assumed to be zero [51,52].

Let the approximate solutions of $\Psi$ , $\theta$ , $\phi$ , $N$ are

$$\Psi=\sum_{i=1}^{3}\Psi_i\xi_i \ ; \ \theta=\sum_{i=1}^{3}\theta_i\xi_i \ ; \ \phi=\sum_{i=1}^{3}\phi_i\xi_i \ ; \ N=\sum_{i=1}^{3}N_i\xi_i$$

where $\xi_i$ are linear interpolating functions obtained for triangular element. Galerkin finite element method for a general element $\Omega_e$ is,

$$\begin{bmatrix}[Q^{11}] & [Q^{12}] & [Q^{13}] & [Q^{14}]\\ [Q^{21}] & [Q^{22}] & [Q^{23}] & [Q^{24}]\\ [Q^{31}] & [Q^{32}] & [Q^{33}] & [Q^{34}]\\ [Q^{41}] & [Q^{42}] & [Q^{43}] & [Q^{44}]\end{bmatrix}\begin{bmatrix}\{\Psi\}\\ \{\mathrm{T}\}\\ \{C\}\\ \{N\}\end{bmatrix}=\begin{bmatrix}\{A_1\}\\ \{A_2\}\\ \{A_3\}\\ \{A_4\}\end{bmatrix}$$

Where

$$Q^{11}=\iint_{\Omega_e}\left[\frac{\partial\xi_j}{\partial X}\frac{\partial\xi_i}{\partial X}+\frac{\partial\xi_j}{\partial Y}\frac{\partial\xi_i}{\partial Y}\right]dXdY \ ;$$

$$Q^{12}=-Ra\iint_{\Omega_e}\left(\xi_j\frac{\partial\xi_i}{\partial X}\right)dXdY \ ;$$

$$Q^{14}=RaRb\iint_{\Omega_e}\left(\xi_j\frac{\partial\xi_i}{\partial X}\right)dXdY \ ;$$

$$Q^{13}=0 \ ; A_1=0 \ ;$$

$$Q^{21}=-Ec\iint_{\Omega_e}\left(\xi_j\frac{\partial\overline{\Psi}}{\partial X}\frac{\partial\xi_i}{\partial X}+\xi_j\frac{\partial\overline{\Psi}}{\partial Y}\frac{\partial\xi_i}{\partial Y}\right)dXdY \ ;$$

$$Q^{22}=\iint_{\Omega_e}\begin{bmatrix}\xi_j\frac{\partial\overline{\Psi}}{\partial Y}\frac{\partial\xi_i}{\partial Y}-\xi_j\frac{\partial\Psi}{\partial X}\frac{\partial\xi_i}{\partial Y}+\frac{\partial\xi_j}{\partial X}\frac{\partial\xi_i}{\partial X}+\frac{\partial\xi_j}{\partial Y}\frac{\partial\xi_i}{\partial Y}\\ -Nt\left(\xi_j\frac{\partial\overline{\theta}}{\partial X}\frac{\partial\xi_i}{\partial X}+\xi_j\frac{\partial\overline{\theta}}{\partial Y}\frac{\partial\xi_i}{\partial Y}\right)\end{bmatrix}dXdY;$$

$$Q^{23}=-Nb\iint_{\Omega_e}\left(\xi_j\frac{\partial\overline{\theta}}{\partial X}\frac{\partial\xi_i}{\partial X}+\xi_j\frac{\partial\overline{\theta}}{\partial Y}\frac{\partial\xi_i}{\partial Y}\right)dXdY \ ;$$

$$Q^{24}=0 \ ; \ A_2=0 \ ;$$

$$Q^{31}=0 \ ; \ Q^{32}=0 \ ;$$

$$Q^{33}=\iint_{\Omega_e}\begin{bmatrix}\frac{\partial\overline{\Psi}}{\partial Y}\xi_j\frac{\partial\xi_i}{\partial X}-\frac{\partial\overline{\Psi}}{\partial X}\xi_j\frac{\partial\xi_i}{\partial Y}+\\ \frac{1}{Le}\left(\frac{\partial\xi_j}{\partial X}\frac{\partial\xi_i}{\partial X}+\frac{\partial\xi_j}{\partial Y}\frac{\partial\xi_i}{\partial Y}\right)\end{bmatrix}dXdY \ ;$$

$$Q^{34}=\iint_{\Omega_e}\frac{\sigma}{Le}\xi_j\xi_i dXdY \ ; \ A_3=0 \ ; \ Q^{41}=0 \ ; \ Q^{42}=0 \ ;$$

$$Q^{43}=0 \ ; \ A_4=0 \ ;$$

$$Q^{44}=\iint_{\Omega_e}\begin{bmatrix}Le\chi\left(\frac{\partial\overline{\Psi}}{\partial Y}\xi_j\frac{\partial\xi_i}{\partial X}-\frac{\partial\overline{\Psi}}{\partial X}\xi_j\frac{\partial\xi_i}{\partial Y}\right)+\\ Pe\xi_j\xi_i\left(\frac{\partial^2\overline{\phi}}{\partial X^2}+\frac{\partial^2\overline{\phi}}{\partial Y^2}\right)+\left(\frac{\partial\xi_j}{\partial X}\frac{\partial\xi_i}{\partial X}+\frac{\partial\xi_j}{\partial Y}\frac{\partial\xi_i}{\partial Y}\right)\end{bmatrix}dXdY;$$

Where

$$\overline{\Psi}=\sum_{j=1}^{3}\overline{\Psi}_j\xi_j \ ; \ \overline{\theta}=\sum_{j=1}^{3}\overline{\theta}_j\xi_j \ ; \ \overline{\phi}=\sum_{j=1}^{3}\overline{\phi}_j\xi_j \ ;$$

Convergence to solution is achieved when the error associated with each unknown between ordered iterations is found to be lower than the convergence condition, $\left|\Phi^{n+1}-\Phi^{n}\right|\le10^{-5}$, where $n$ is iteration number and $\Phi$ stands for $\Psi,\theta,\phi$ and $N$. Grid size independency check is implemented as shown in Table 1. The grid size check infers that a mesh of $101\times101$ is convenient to study bioconvection. The validation of present problem is observed when viscous dissipation and microorganisms are absent. The computed data are matched up to the results available in literature and observed to be in good agreement (see Table.2).

## 4 Results and discussion

The calculated results have been exhibited for diverse values of Rayleigh number of bioconvection $(20\le Rb\le50)$, Brownian motion $(0.1\le Nb\le0.3)$,

Table 1 — Grid independency against the average Nusselt numbers for Ra=300, Rb=10, Nb=0.1, Nt=0.1, Pe=0.1, Le=1 and Ec=0.1.

| Grid size X×Y | Average Nusselt number $Nu_{avg}$ |
|---|---|
| 21×21 | $3.0247\times10^{-2}$ |
| 41×41 | $2.6524\times10^{-2}$ |
| 61×61 | $2.5302\times10^{-2}$ |
| 81×81 | $2.5186\times10^{-2}$ |
| 101×101 | $2.4992\times10^{-2}$ |
| 121×121 | $2.4981\times10^{-2}$ |

thermophoretic force $(0.1 \le Nt \le 0.3)$, Eckert number $(0.01 \le Ec \le 0.3)$, Lewis number $(0.1 \le Le \le 1)$ and Peclet number $(0.1 \le Pe \le 1)$.

Table 2 — Comparison of the Nusselt numbers at the hot wall.

| | Ra=10 | Ra=100 | Ra=1000 | Ra=10000 |
|---|---|---|---|---|
| Goyeau *et al.* [53] | — | 3.110 | 13.470 | — |
| Walker and Homsy [54] | Nil | 3.097 | 12.96 | 51.0 |
| Baytas and Pop [55] | 1.079 | 3.16 | 14.06 | 48.33 |
| Revnic *et al.* [56] | — | — | 13.664 | — |
| Sheremet and Pop [17] | 1.079 | 3.115 | 13.667 | 48.823 |
| Present results | 1.0791 | 3.1147 | 13.6453 | 48.7451 |

**4.1 Effect of Eckert number**

Fig. 2 presents the surface plots of stream function, temperature, oxygen concentration, microorganism concentration for Eckert number $Ec = 0.1, 0.3$. The streamlines produce a cell occupying whole enclosure in counterclockwise rotation (upward direction) when $Ec = 0.1$. The stream function attains maximum value $\Psi_{max} = 1.54$ at the center of the enclosure. As Eckert number increases to $Ec = 0.3$, the flow cell splits into two cells, which are extended in opposite directions. The range of the stream function is $-0.92 \le \Psi \le 1.05$.

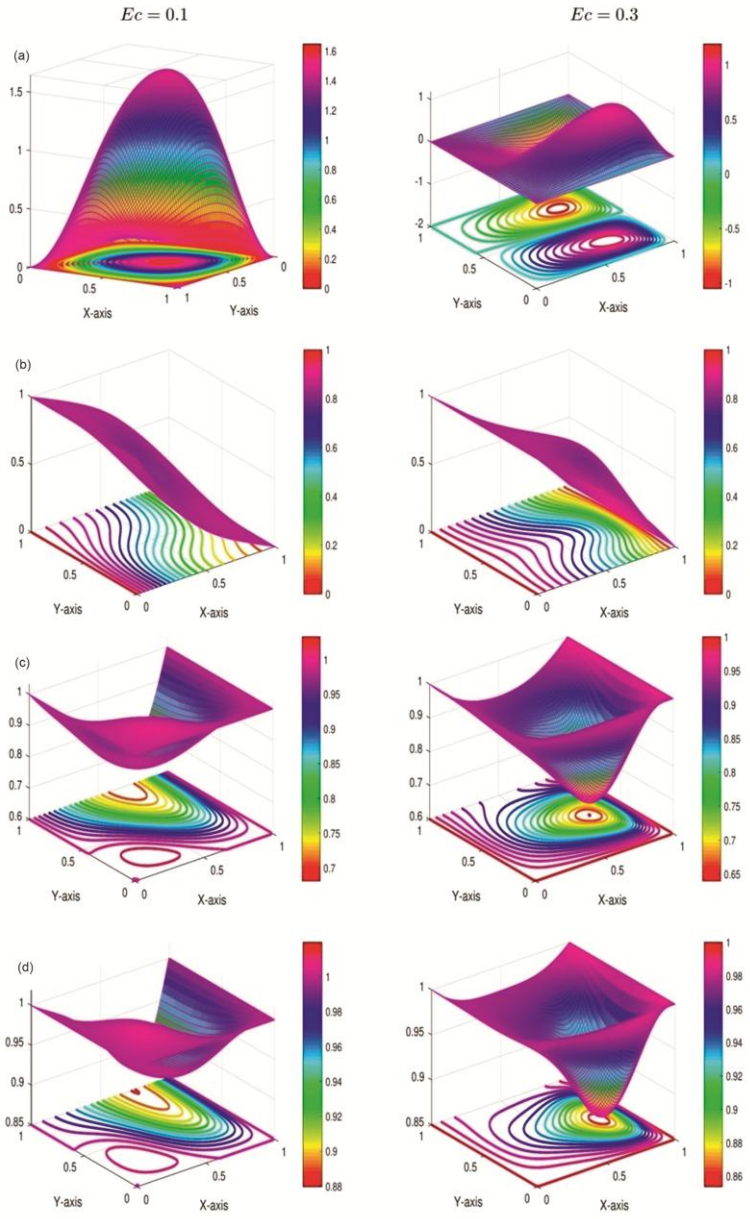


Fig. 2 — Surface plots of stream function, temperature, concentrations of oxygen and microorganisms for Ra=20, Rb=10, Nb=0.1, Nt=0.1, Pe=0.1, Le=1 and (a) Ec=0.1 (b) Ec=0.3.

The isotherms are formed parallel to hot wall when $Ec = 0.1$. As $Ec$ enhances the isotherms are stratified at center describing the convection form of heat transfer. This is due to the reason that raise in Eckert number squeezes the surface plot of temperature towards the cold wall. The rate of heat transfer is high for larger values of $Ec$.

The steepness of the surface plot of oxygen concentration indicates that the gradient of oxygen concentration is more at the cold wall, and it is less at the hot and bottom walls of the enclosure. When $Ec = 0.1$, a semi vortex is produced at center, due to less density at the center of the enclosure. Low density region is also formed at the top wall of the enclosure due to boundary conditions at the top and bottom wall. As the Eckert number increases to $Ec = 0.3$, density of oxygen increases at the top wall of enclosure and the vortex indicating low density region shifts towards cold wall. An eddy is observed at the bottom left wall of the enclosure and that is disappeared with the boost in viscous dissipation. However, Eckert number increases the depth of the vortex of oxygen concentration.

A low strength eddy is found near the hot wall and a downward pointing vortex is produced near the cold wall of the enclosure for the Eckert number $Ec = 0.1$. This shows that the density of oxytactic microorganisms is high near hot wall and gradient of microorganisms is observed at the cold and bottom wall. Due to the boundary condition of the problem an opened semi vortex towards top wall is appeared. When the Eckert number increased to $Ec = 0.3$ gradient of oxytactic microorganism is also observed at the top wall. A deeper cell of microorganism density is found at the cold wall. The increase in the viscous dissipation stabilizes the microorganisms density in the enclosure and a steeper low-density region is formed at the cold wall.

#### 4.2 Effect of Brownian motion

Fig. 3 presents the surface plots of stream function, temperature, oxygen concentration, microorganism concentration for Brownian motion parameter $Nb = 0.1, 0.3$. A single flow cell occupying the entire enclosure is formed when the Brownian motion parameter $Nb = 0.1$. The boost in the Brownian motion decreases flow intensity of stream function from $\Psi_{max} = 1.14$ to $\Psi_{max} = 0.63$. This is due to the increased random movement of the nanoparticles present in fluid containing ox tactic microorganisms.

An insignificant impact of Brownian motion is observed on distribution of temperature in the enclosure. The rate of heat transfer is reduced slightly with the boost in Nb.

An opened semi vortex towards top wall is observed in the surface plot of oxygen concentration. When $Nb = 0.1$ less gradient of oxygen density at the left(hot) wall, bottom wall and right(cold) wall is noticed. As the Brownian motion increased to $Nb = 0.3$ high gradient of oxygen density is observed at the aforesaid walls and the depth of the vortex is reduced. The values of oxygen isoconcentrations ranges between $1 \leq \emptyset \leq 0.728$ for Nb=0.1 and $1 \leq \emptyset \leq 0.8664$ for Nb=0.3.

A semi vortex opened towards top wall is appeared in the surface plot of oxytactic microorganisms. It is observed from the figure that the Brownian motion decreases the depth of the vortex, which indicates the stable distribution of microorganisms. This is due to the interaction between the swimming of oxytactic microorganisms and random motion of nanoparticles in the enclosure. The values of microorganisms isoconcentrations ranges between $1 \leq N \leq 0.931$ for Nb=0.1 and $1 \leq N \leq 0.962$ for $Nb = 0.3$.

#### 4.3 Effect of thermophoresis

Fig. 4 presents the surface plots of stream function, temperature, oxygen concentration, microorganism concentration for Brownian motion parameter $Nt = 0.1, 0.3$. When Nt=0.1, single cell of flow in the clockwise direction in the enclosure is formed and the flow strength ranges between $0 \leq \Psi \leq 0.798$. As the thermophoretic parameter increases to Nt=0.3 an eddy is formed in the anticlockwise direction and the flow strength in the clock direction enhances between $-0.13 \leq \Psi \leq 1.497$. This is due to the interaction of nanoparticles with other species/molecules in the fluid in response to the temperature gradient.

When Nt=0.1 the isotherms are parallel to the hot wall linear rate of heat transfer is observed. When Nt=0.3 the isotherms stratified horizontally indicating the higher rate of heat transfer.

The density of oxygen is highest at the left(hot) wall, bottom wall and right(cold) wall when Nt=0.1. The isoconcentrations of oxygen shows that the density of oxygen decreases gradually from aforesaid walls to the centre of the enclosure. With the increase in the thermophoretic force an interaction among nanoparticles, oxygen particles and microorganisms takes place and a tiny cell of isoconcentrations of

oxygen in the anticlockwise direction, is formed. The range of oxygen density is $1 \le \phi \le 0.75$ when Nt=0.1 and $1.12 \le \phi \le 0.27$ when Nt=0.3. The boundary layer of oxygen concentration decreases with the increase in Nt.

When Nt=0.1, a vortex indicating low density region of oxytactic bacteria is formed at the centre of the enclosure. High density region of oxytactic microorganisms is formed at the bottom wall and hot wall. As the thermophoretic force increases a rapid moment of microorganisms towards cold wall takes place and a reverse flow is occurred at the left of bottom wall. Due to this a strong cell of microorganisms is formed and the strength of semi vortex at the centre decreased. The effect of Nt on the

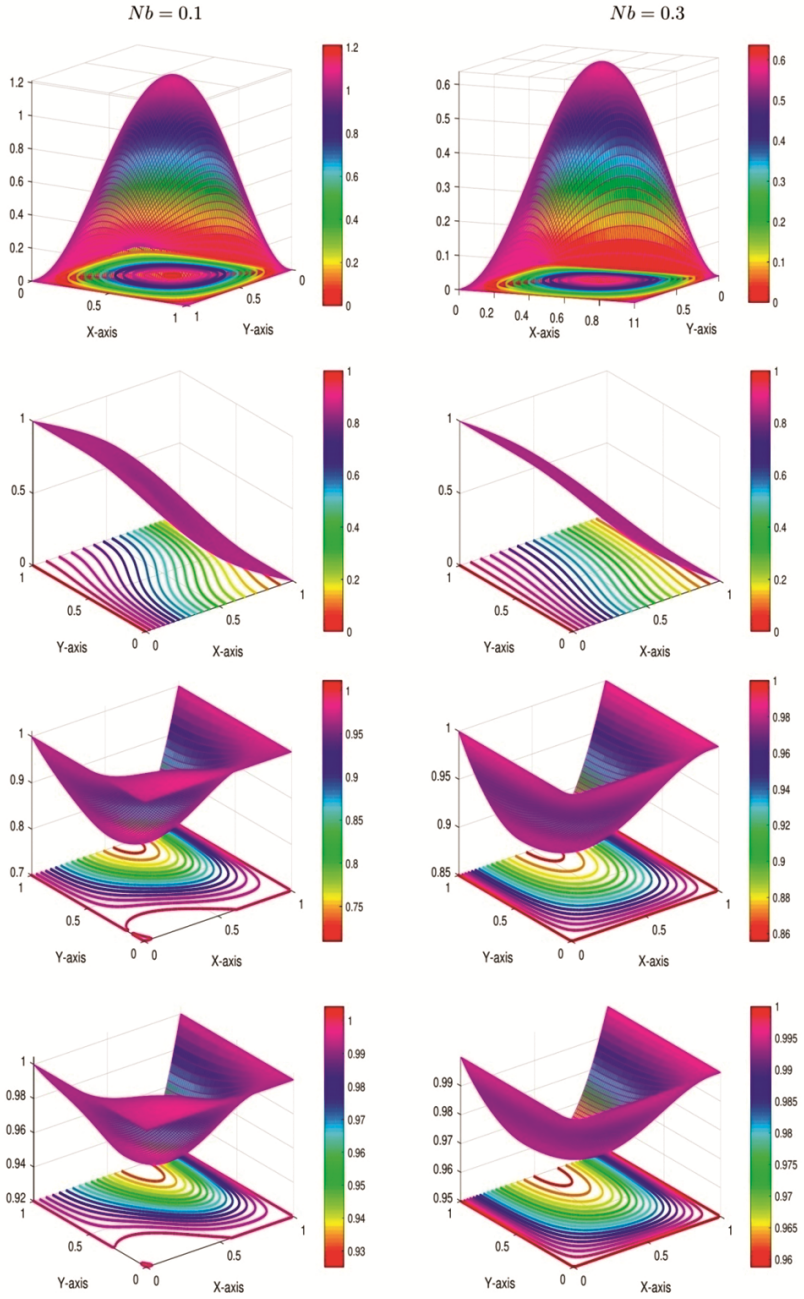


Fig. 3 — Surface plots of stream function, temperature, concentrations of oxygen and microorganisms for Ra=20, Rb=10, Nt=0.1, Pe=0.1, Ec=0.01, Le=1 and (a) Nb=0.1 (b) Nb=0.3.

boundary layer of density of microorganisms is less when compared to that of oxygen.

**4.4 Effect of Peclet number**

Fig. 5 shows the surface plots of stream function, temperature, oxygen concentration and microorganisms concentration for Pe=0.2, 0.8. Peclet number increases the flow intensity greatly. The range of stream function is $1 \le \Psi \le 0.252$ when Pe=0.2 and $0 \le \Psi \le 1.554$ when Pe=0.8. Peclet number increases rate of heat transfer. With the boost in Peclet number the semi vortex which is opened towards top wall, produces an eddy in the opposite direction. The same

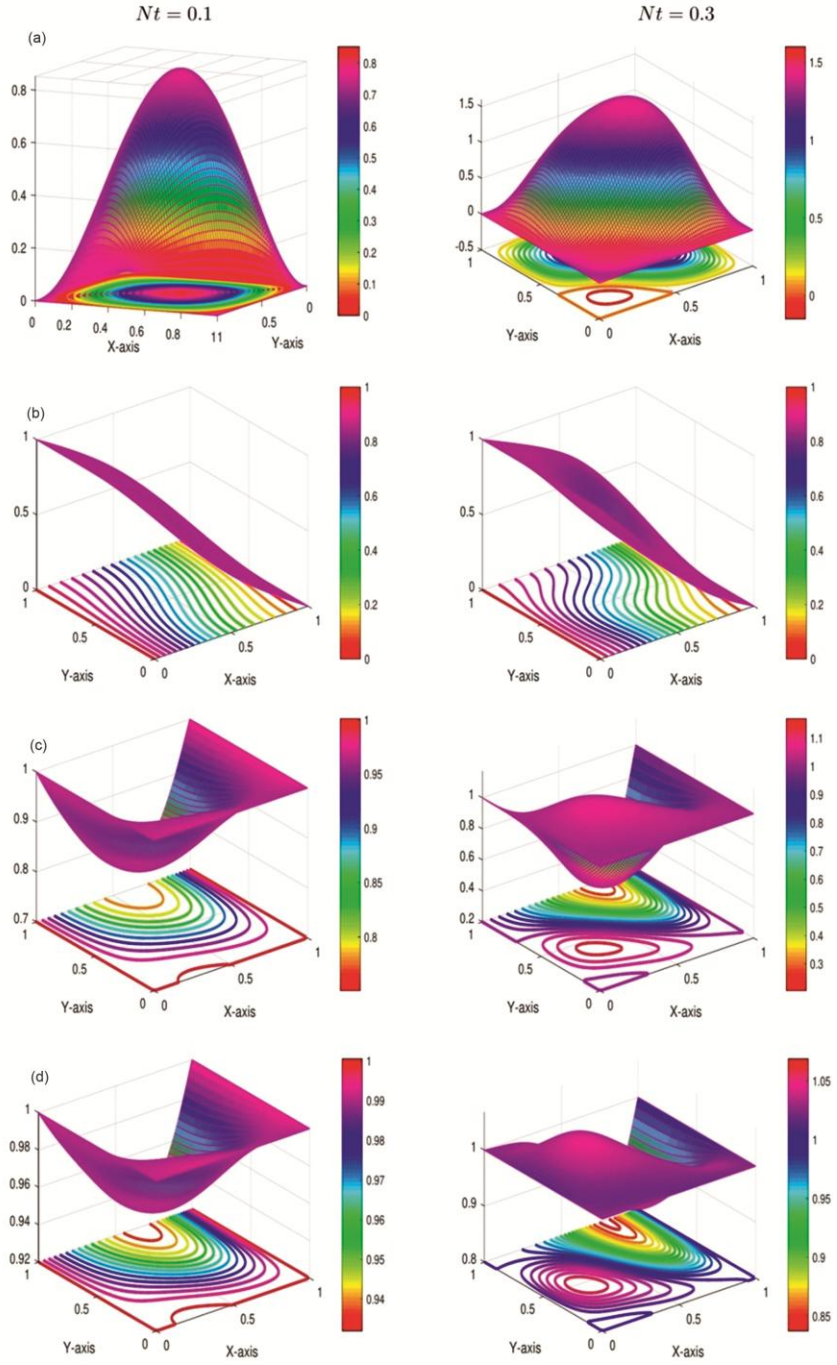


Fig. 4 — Surface plots of stream function, temperature, concentrations of oxygen and microorganisms for Ra=20, Rb=10, Nb=0.1, Pe=0.5, Ec=0.01, Le=1 and (a) Nt=0.1 (b) Nt=0.3.

trend is observed with the surface plots of concentration of oxytactic microorganisms, because of the dominance of the diffusivity of motile organisms. It is observed that boundary layer thickness of both concentrations of oxygen and microorganisms is decreased with the increase in Peclet number.

**4.5 Effect on Average Nusselt number, Sherwood numbers of Oxygen density and microorganisms density**

Fig. 6 reveals the effect of Eckert number versus Peclet number on average Nusselt number $Nu_{avg}$, Sherwood number of oxygen density $Sh_{avg}$ and Sherwood number of microorganisms $Nn_{avg}$. It is noticed that $^{Nu_{avg}}$ is increasing function of both Eckert

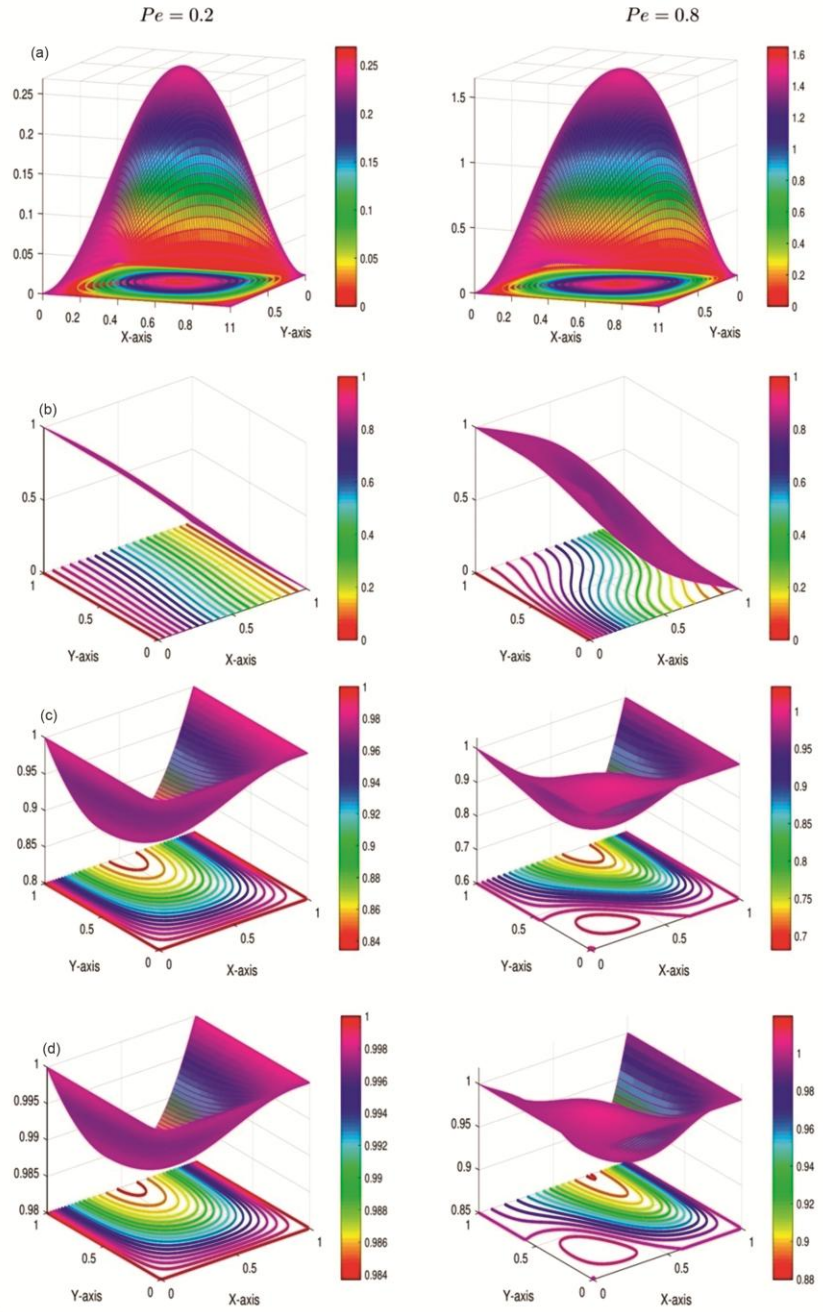


Fig. 5 — Surface plots of stream function, temperature, concentrations of oxygen and microorganisms for Ra=20, Rb=10, Nb=0.1, Nt=0.1, Le=0.1, Ec=0.01 and (a) Pe=0.2 (b) Pe=0.8.

number and Peclet number. While reverse trend is observed in case of $Sh_{avg}$ and $Nn_{avg}$.

The influence of bioconvection Rayleigh number against Lewis number on average Nusselt number $Nu_{avg}$, Sherwood number of oxygen density $Sh_{avg}$ and Sherwood number of microorganisms $Nn_{avg}$ is shown in Fig. 7. Lewis number decreases $Nu_{avg}$. This effect is pronounced with higher bioconvection Rayleigh number. Lewis number increases $Sh_{avg}$. This effect is

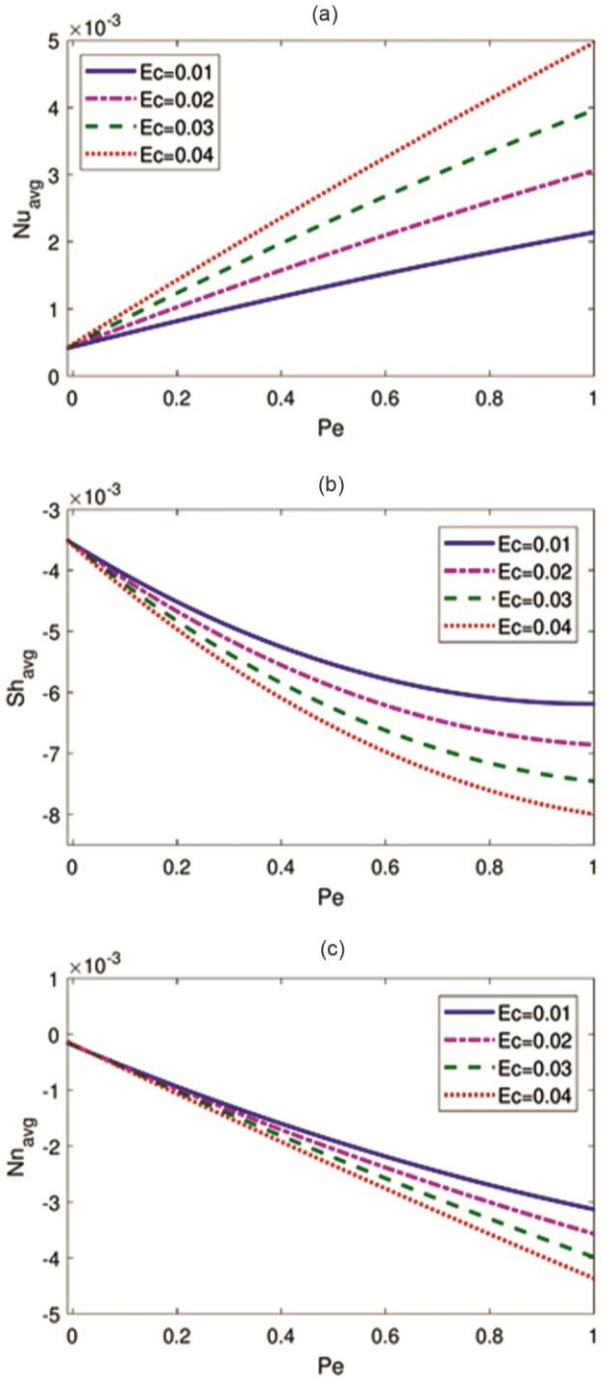


Fig. 6 — Effect of Eckert number vs. Peclet number on (a) average Nusselt number (b) average Sherwood number of oxygen concentration (c) average Sherwood number of microorganisms concentration.

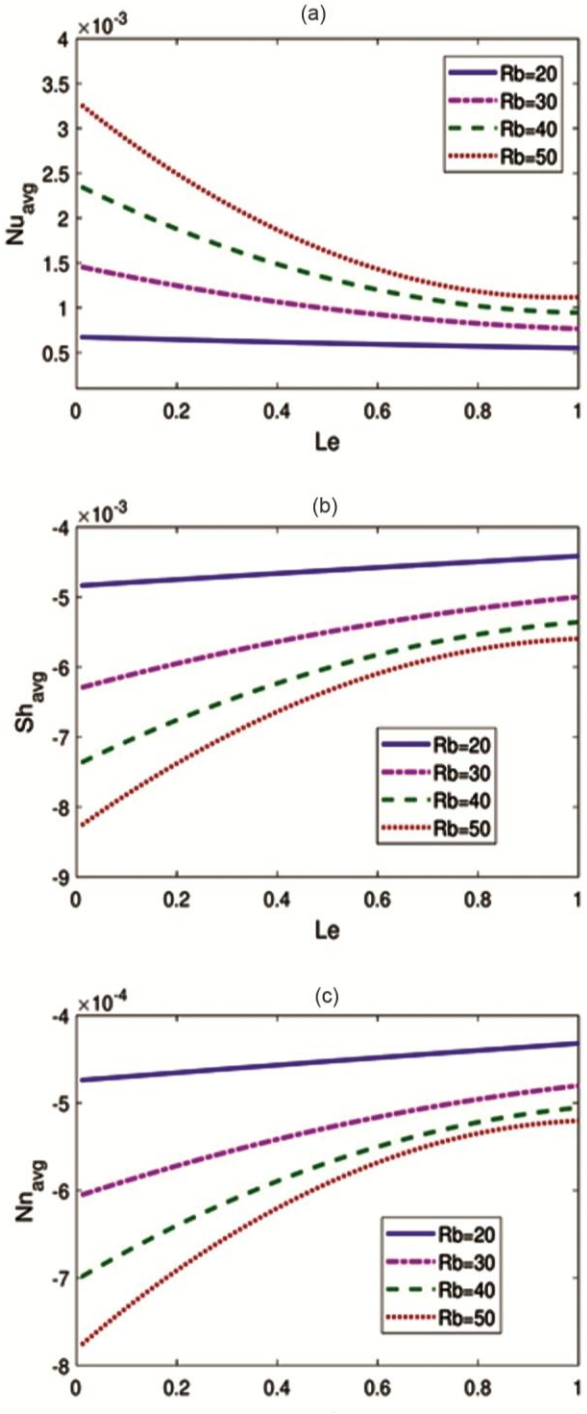


Fig. 7 — Effect of bioconvection Rayleigh number vs. Lewis number on (a) average Nusselt number (b) average Sherwood number of oxygen concentration (c) average Sherwood number of microorganisms concentration.

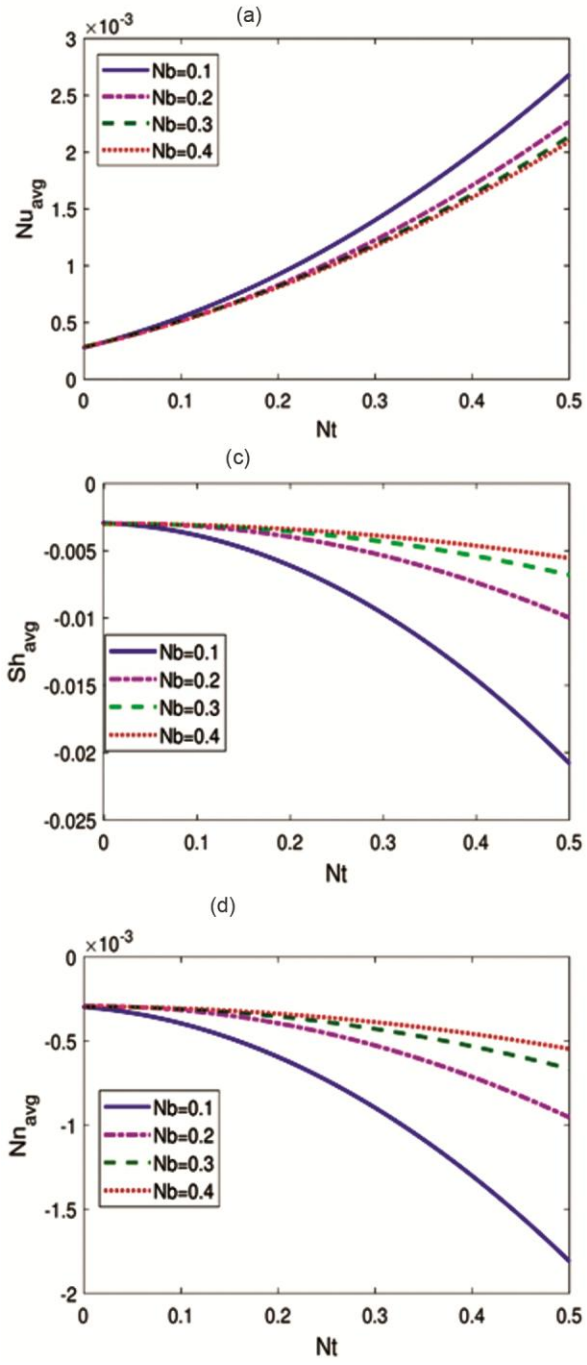


Fig. 8 — Effect of Brownian motion vs. thermophoretic parameter on (a) average Nusselt number (b) average Sherwood number of oxygen concentration (c) average Sherwood number of microorganisms concentration.

pronounced with lower bioconvection Rayleigh number. The similar effect on $Nn_{avg}$ is observed.

The impact of Brownian motion vs. thermophoretic parameter on average Nusselt number $Nu_{avg}$, Sherwood number of oxygen density $Sh_{avg}$ and Sherwood number of microorganisms $Nn_{avg}$ is shown in Fig. 8. $Nu_{avg}$ reduces with the raise in Brownian motion and it enhances significantly with the increase in thermophoretic parameter. The opposite trend is observed in case of $Sh_{avg}$ and $Nn_{avg}$.

## 5 Conclusion

In this paper, bioconvection in a square enclosure containing nanofluid-suspension of oxytactic microorganisms associated with viscous dissipation is investigated. The non-dimensional form of governing partial differential equations is obtained and solution is found by means of finite element method. The surface plots of streamlines, isotherms, is concentrations of oxygen and microorganisms, Nusselt number and Sherewood numbers of oxygen density and density of oxytactic microorganisms were explored graphically. The key conclusions are:

- The strength of flow is enhanced with Eckert number, thermophoretic parameter and Peclet number. And it is decreased with Brownian motion parameter.
- The rate of heat transfer is pronounced with Eckert number, thermophoretic parameter and Peclet number. And it is reduced with Brownian motion parameter.
- Eckert number reduces oxygen density profile in the enclosure but enhances at the top wall. Brownian motion enhances the oxygen density profile. Thermophoretic force and Peclet number enhance the boundary layer thickness of oxygen density and cause a reverse flow to occur.
- Eckert number reduces the concentration profile of oxytactic microorganisms in the enclosure but boosts at the top wall. Brownian motion increases the concentration of microorganisms. Thermophoretic force enhances the boundary layer of microorganisms density and causes for a strong reverse flow in the enclosure. Peclet number stabilizes the concentration profile of oxytactic bacteria.
- Brownian motion and Lewis number reduces the average Nusselt number $Nu_{avg}$ and enhances the average Sherwood number of oxygen density $Sh_{avg}$ and average Sherwood number of microorganisms density $Nn_{avg}$. However, thermophoretic parameter, bioconvection Rayleigh number, Peclet number and Eckert number enhance $Nu_{avg}$ and reduce both $Sh_{avg}$ and $Nn_{avg}$.

## Acknowledgement

One of the authors Naikoti Kishan acknowledges the UGC for financial support under the DST-PURSE Programme of Osmania University, Hyderabad-7, T.S

## References

1 Nield D A & Bejan A, *Convection in Porous Media*, (Springer New York, 2013).
2 Vafai K, *Hand Book of Porous Media*, 2nd Edn New York, (2005).
3 Pop I & Ingham D B, *Convective heat transfer: mathematical and computational modelling of viscous fluids and porous media*, (Elsevier, 2001).
4 Rahman M M, Pop I & Saghir M Z, *Int J Heat Mass Transfer*, 129 (2019) 198.
5 Shekar B C, Kishan N & Chamkha A J, *J Porous Media*, 19 (2016) 669.
6 Sekhar B C, Kishan N & Haritha C, *J Thermophys Heat Transfer*, 31 (2017) 549.
7 Balla C S, Kishan N, Gorla R S R & Gireesha B J, *Ain Shams Eng J*, 8 (2017).
8 Shekar B C, Haritha C & Kishan N, *J Proc Mech Eng*, 233 (2018) 474.
9 Childress S, Levandowsky M & Spiegel E A, *J Fluid Mech*, 69 (1975) 591.
10 Pedley T J, Hill N A & Kessler J O, *J Fluid Mech*, 195 (1988) 223.
11 Hill N A, Pedley T J & Kessler J O, *J Fluid Mech*, 208 (1989) 509.
12 Hillesdon A J, Pedley T J & Kessler J O, *Bull Math Biol*, 57 (1995) 299.
13 Hillesdon A J & Pedley T J, *J Fluid Mech*, 324 (1996) 223.
14 Becker S M, Kuznetsov A V & Avramenko A A, *Fluid Dynamics Res*, 35 (2004) 323.
15 Kuznetsov A V, *Int Commun Heat Mass Transfer*, 32 (2005) 991.
16 Kuznetsov A V, *Theor Comput Fluid Dynamics*, 19 (2005) 287.
17 Sheremet M A & Pop I, *Trans Porous Media*, 103 (2014) 191.
18 Kuznetsov A V, *Eur J Mech - B/Fluids*, 25 (2006) 223.
19 Ahmed S, Oztop H, Mansour M & Abu-Hamdeh N, *Therm Sci*, 22 (2018) 2711.
20 Choi S U S & Eastman J A, *Enhancing thermal conductivity of fluids with nanoparticles*. (1995).
21 Xuan Y & Roetzel W, *Int J Heat Mass Transfer*, 43 (2000) 3701.
22 Khanafer K, Vafai K & Lightstone M, *Int J Heat Mass Transfer*, 46 (2003) 3639.
23 Buongiorno J, *J Heat Mass Transfer*, 128 (2005) 240.
24 Tiwari R K & Das M K, *Int J Heat Mass Transfer*, 50 (2007) 2002.
25 Sheikholeslami M, Ganji D D & Rashidi M M, *J Magn Magn Mater*, 416 (2016) 164.
26 Fan X, Chen H, Ding Y, Plucinski P K & Lapkin A A, *Green Chem*, 10 (2008) 670.
27 Li H, Liu S, Dai Z, Bao J & Yang X, *Sensors*, 9 (2009) 8547.
28 Huh D, *Science*, 328 (2010) 1662.
29 Do K H & Jang S P, *Int J Heat Mass Transfer*, 53 (2010) 2183.
30 Ebrahimi S, Sabbaghzadeh J, Lajevardi M & Hadi I, *Int J Heat Mass Transfer*, 46 (2010) 549.
31 Tham L, Nazar R & Pop I, *Int J Heat Mass Transfer*, 62 (2013) 647.
32 Raz O & Avron J E, *New J Phys*, 9 (2007) 437.
33 Weibel D B, *Proceedings of the National Academy of Sciences*, 102 (2005) 11963.
34 Desouky S M, Abdel-Daim M M, Sayyouh M H & Dahab A S, *J Petrol Sci Eng*, 15 (1996) 309.
35 Stewart T L & Kim D S, *Biochem Eng J*, 17 (2004) 107.
36 Saranya S & Radha K V, *Polymer-Plastics Technol Eng*, 53 (2014) 1636.
37 Bég O A, Prasad V R & Vasu B, *J Mech Med Biol*, 13 (2013).
38 Balla C S, Haritha C, Naikoti K & Rashad A M, *Int J Numer Meth Heat Fluid Flow* 29 (2019) 1448.
39 Kefene M Z, Makinde O D & Enyadene L G, *Indian J Pure Appl Phys*, 58 (2020) 892.
40 Chaudhary S, Chaudhary S & Choudhary M, *Indian J Pure Appl Phys*, 58 (2020) 71.
41 Mahajan R L & Gebhart B, *Int J Heat Mass Transfer*, 32 (1989) 1380.
42 Nakayama A & Pop I, *Int Commun Heat Mass Transfer*, 16 (1989) 173.
43 Balla C S & Naikoti K, *Alex Eng J*, 54 (2015) 661.
44 Haritha C, Shekar B C & Kishan N, *J Nanofluids*, **7** (2018) 928.
45 Aziz A, Khan W A & Pop I, *Int J Thermal Sci*, 56 (2012) 48.
46 Shaw S, Motsa S S & Sibanda P, *Heat Transfer-Asian Res*, 47 (2018) 718.
47 Gireesha B J, Kumar K G, Rudraswamy N G & Manjunatha S, *Defect Diffus Forum*, 388 (2018) 114.
48 Hady F M, Mahdy A, Mohamed R A & Zaid O A A, *World J Mech*, 06 (2016) 505.
49 Uddin M J, Khan W A & Ismail A I, *J Nanoeng Nanosyst*, 227 (2012) 11.
50 Khan U, Ahmed N & Mohyud-Din S T, *SpringerPlus*, 5 (2016).
51 Kishan N & Shekar B C, *J Appl Sci Eng*, 18 (2015) 143.
52 Balla C S & Naikoti K, *Int J Eng Sci Technol*, 18 (2015) 543.
53 Goyeau B, Songbe J P & Gobin D, *Int J Heat Mass Transfer*, 39 (1996) 1363.
54 Walker K L & Homsy G M, *J Fluid Mech*, 87 (1978) 449.
55 Baytas A C & Pop I, *Int J Heat Mass Transfer*, 42 (1999) 1047.
56 Revnic C, Grosan T, Pop I & Ingham D B, *Int J Thermal Sci*, 48 (2009) 1876.